

Ultrasonic nucleation of bioactive glass particles

Michiel Postema^{1,2†*}, Craig S. Carlson^{1,2}, Nicole Anderton¹, Hu Xinyue³, Momoka Yamasaku³, Laeticia Petit⁴, Jonathan Massera¹, and Nobuki Kudo³
 (¹BioMediTech, Fac. Med. & Health Technol., Tampere Univ., Finland; ²School Elec. & Inform. Eng., Univ. Witwatersrand, Johannesburg, South Africa; ³Fac. Inform. Sci. & Technol., Hokkaido Univ., Japan; ⁴Photonics Lab., Fac. Eng. Nat. Sci., Tampere Univ., Finland)

1. Introduction

Bioactive glass is a class of biomaterials, generally used in bone regeneration, able to precipitate hydroxyapatite, upon immersion in physiological medium.¹⁾ The precipitation of a reactive layer promotes cells attachment while the release of ions triggers signalling pathways leading not cell proliferation and differentiation, conferring this biomaterial osteostimulative properties.¹⁾ While silicate bioactive glasses such as S53P4 and 45S5 are often used clinically, much research has been devoted to borosilicate glasses, since they not only promote osteogenesis but also angiogenesis.²⁾

A commonly studied bioactive glass is 13-93B20.³⁾ Despite its density of 2.60 g cm^{-3} at room temperature, small but not negligible quantities of 13-93B20 have been observed to float in aqueous media, rather than to sink. It has been hypothesised that microscopic gas bubbles entrapped in the particles are causing this undesired feature. The purpose of this study was to evaluate this hypothesis by subjecting 13-93B20 particles to ultrasound to trigger a release mechanism and to quantify any effects thereof.

2. Materials and Methods

Borosilicate bioactive glass 13-93B20 was prepared using analytical grade K_2CO_3 (Alfa Aesar, Ward Hill, MA, USA), Na_2CO_3 , $\text{NH}_4\text{H}_2\text{PO}_4$, $(\text{CaHPO}_4)(2(\text{H}_2\text{O}))$, CaCO_3 , MgO , H_3BO_3 (Sigma Aldrich, St Louis, MO, USA), and Belgian quartz sand, as reported previously.³⁾ Briefly, 60 g of glass was melted in a Pt crucible, in air, at 1450°C for 3 h. After casting in a graphite mould, the glass was annealed at 550°C , to remove any residual stress. Successively, the glass block was crushed and sieved to obtain particles with sizes $< 38 \mu\text{m}$.

Quantities of 5 mg of 13-93B20 bioactive glass particles were stirred through 5 ml of degassed distilled water (FUJIFILM Wako Pure Chemical Corporation, Chuo-ku, Osaka, Japan). For each experiment, 200 μl of this dispersion was pipetted into a cylindrical compartment of 8-mm diameter

and 2-mm height before being closed with an $18 \times 18 \text{ mm}$ Thickness No. 1 Micro Cover Glass (Matsunami Glass Ind., Ltd., Kishiwada-shi, Osaka, Japan) and sealed with No.600M cloth tape (Sekisui Chemical Co., Ltd., Kita-ku, Osaka, Japan).

The compartment was part of a $244 \times 145 \times 76\text{-mm}^3$ Perspex container that was positioned on top of an Eclipse Ti inverted microscope (Nikon Corporation, Minato-ku, Tokyo, Japan) with a Plan Apo $10 \times / 0.45$ objective lens (Nikon), a $1.5 \times$ internal zoom, and a G-2A filter. The microscope was attached to an HPV-X2 high-speed camera (Shimadzu, Nakagyo-ku, Kyoto, Japan), operating at frame rates equal to ten million frames per second during sonication. The driving system was identical to the one previously described:⁴⁾ a 3-cycle pulse at a 1-MHz centre frequency was generated by an AFG320 arbitrary function generator (Sony-Tektronix, Shinagawa-ku, Tokyo, Japan), amplified by a UOD-WB-1000 wide-band power amplifier (TOKIN Corporation, Shiroishi, Miyagi, Japan), and fed into a custom-built transducer.⁵⁾ The signal amplitude of 5 V corresponded to a peak-negative pressure of 1.2 MPa.

A total number of ten high-speed videos was recorded, each consisting of 256 frames. These frames were imported into the matrix laboratory MATLAB[®] (The MathWorks, Inc., Natick, MA, USA) for further processing. For each particle i , the visual particle surface area A_i was measured, after which the effective radius $d_{i-} = (4A_i/\pi)^{1/2}$ was computed.

3. Results and Discussion

Fig. 1 shows still frames of 16 bioactive glass particles that were floating and 145 that had sunk to the bottom of the sonication compartment, pre-sonication as well as 208 post-sonication. The ratio of particles on the surface and particles on the bottom was 1:11. Indeed, a small but not negligible subset of the particles appeared to float rather than sink. Post-sonication, the particles that had been floating pre-sonication were no longer visible, whilst other, visibly smaller particles appeared to have sunk to the bottom.

^{†*} Correspondence to: michiel.postema@tuni.fi

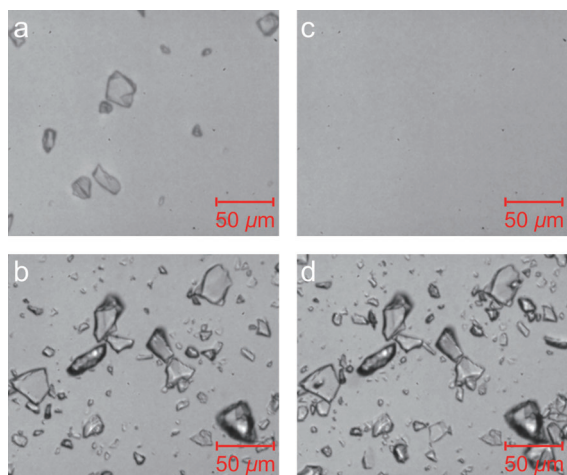


Fig. 1 Pre-sonication (a,b) and post-sonication (c,d) brightfield microscopy images at a 15× magnification 13-93B20 particles at the top (a,c) and bottom (b,d) surfaces of the sonication compartment.

Fig. 2 shows the effective diameter histograms for floating and sunken 13-93B20 particles pre-sonication, as well as sunken particles post-sonication. The effective diameters post-sonication approximated the cumulative pre-sonication histograms, except for a higher number of particles <8 μm. This higher count may be attributed to disruptive effects of the ultrasound (not shown).

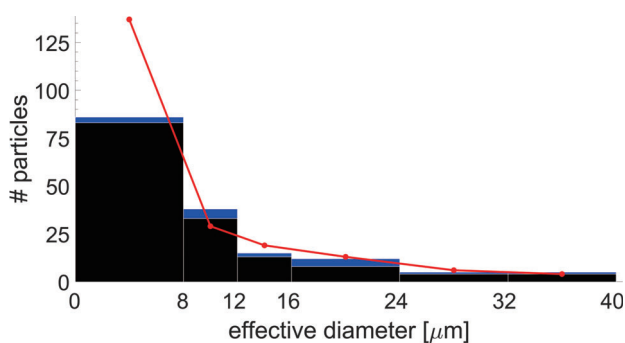


Fig. 2 Effective diameter histograms for floating (blue) and sunken 13-93B20 particles (black) pre-sonication, and sunken particles post-sonication (red).

Fig. 3 shows selected highspeed video frames during sonication. Two particles were observed to nucleate, followed by coalescence of the newly formed bubbles and undergoing explosive growth. In subsequent frames, the source particles were observed to move and shift out of optical focus.

It must be noted that, although nucleation and explosive growth have been observed with microscopic hydrophobic particles at similar acoustic amplitudes,⁶⁾ the pressures used in this study were less than the threshold for inertial cavitation to occur.⁷⁾ Therefore, we may attribute the phenomena

observed to the presence of cavitation nuclei inside or on the surface of the glass particles. This attribution is confirmed by the nucleation footage (cf. Fig. 3b).

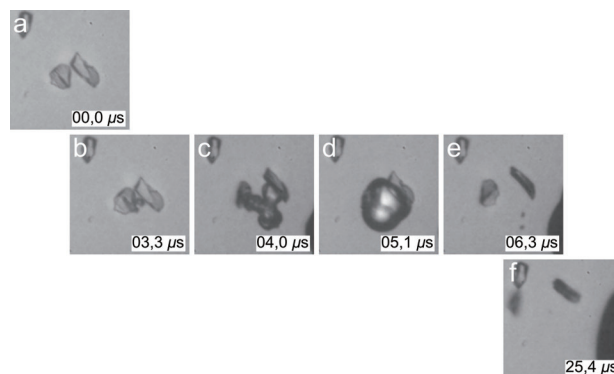


Fig. 3 Selected frames before (a), during (b–e), and after sonication (f). Timestamps have been added to the lower right corners. Exposure times were 100 ns per frame. Each frame corresponded to a 100×100-μm² area.

4. Conclusions

The highspeed photography footage strengthens the hypothesis that some bioactive glass particles contained gas that was released owing to sonication. A detailed study on the release mechanism is required before the hypothesis can be evaluated.

Acknowledgements

This work was supported by JSPS KAKENHI, Grant Nos. JP17H00864 and JP20H04542, by the National Research Foundation of South Africa, Grant No. 127102, and by the Academy of Finland, Grant No. 340026.

References

- 1) L. L. Hench, *J. Mater. Sci. Mater. Med.* **17**, 967 (2006).
- 2) M. Ojansivu, A. Mishra, S. Vanhatupa, M. Juntunen, A. Larionova, J. Massera, and S. Miettinen, *PloS One* **13**, e0202740 (2018).
- 3) A. Houaoui, A. Szczodra, M. Lallukka, L. El-Guermah, R. Agniel, E. Pauthe, J. Massera, M. Boissiere, *Biomolecules* **11**, 444 (2021).
- 4) N. Anderton, C. S. Carlson, A. T. Poortinga, H. Xinyue, N. Kudo, and M. Postema, *Jpn. J. Appl. Phys.* **62** 018001 (2023).
- 5) N. Kudo, *IEEE Trans. Ultrason. Ferroelect. Freq. Control* **64**, 273 (2017).
- 6) C. S. Carlson, R. Matsumoto, K. Fushino, M. Shinzato, N. Kudo, and M. Postema, *Jpn. J. Appl. Phys.* **60**, SDDA06 (2021).
- 7) J. Yasuda, A. Asai, S. Yoshizawa, and S.-i. Umemura, *Jpn. J. Appl. Phys.* **52**, 07HF11 (2013).